

## Crystal Engineering | Hot Paper |

 High-pressure Nucleation of Low-Density Polymorphs\*\*Szymon Sobczak, Paulina Ratajczyk, and Andrzej Katrusiak\*<sup>[a]</sup>

**Abstract:** New polymorphs  $\beta$  and  $\gamma$  of bis-3-nitrophenyl disulphide, crystallized above 0.3 GPa, are less dense than the ambient-pressure polymorph  $\alpha$ . This counterintuitive density relation results from the high-entropy nucleation and subsequent kinetic crystallization. The work performed by pressure compensates the high entropy and temperature product, substantiated in varied conformers and increased chemical potential. Pressure-increased viscosity promotes the kinetic polymorphs, in accordance with empirical Ostwald's rule of stages. It contrasts to mechanochemical techniques, favouring high-density polymorphs.

The rational control over polymorphic forms of organic compounds is one of the challenges of materials sciences, modern chemistry, and related technologies.<sup>[1–3]</sup> Apart from the environment (solvent, pressure, temperature, composition, evaporation rate, etc.) also the intrinsic features (intra- and intermolecular interactions of conformers, mesmeric forms, tautomers, solvates etc.) need to be taken into account for designing the robust process aimed at the desired specific polymorph.<sup>[2,4–6]</sup> Such precise technologies are applied for obtaining required forms of pharmaceuticals, pesticides, food, plastics, dyes and various other products. Despite a considerable progress in the crystal-structure prediction,<sup>[7–10]</sup> in most cases the experimental screening provides the most reliable information about polymorphs of compounds. Generally, the crystal form results from the initial aggregation of molecules, either primary or secondary nucleation, and from the time-dependent crystal growth, either dynamic or kinetic.<sup>[1,2,5,11]</sup> The dynamic crystallizations proceed slowly, in the nearly equilibrated systems, whereas the

kinetic crystallizations take place off the thermodynamic equilibrium, for example in quickly cooled molten or dissolved compounds. The dynamic and kinetic crystallizations often lead to different polymorphs. Some compounds, irrespective of thermodynamic conditions of their nucleation, have been obtained in only one crystalline form, for example naphthalene and CS<sub>2</sub>.<sup>[12,13]</sup> An interesting example of high-pressure crystallization controlled by the seeds obtained at normal conditions for promoting the growth of low-density polymorphs was described for chlorpropamide,<sup>[14]</sup> a reverse approach of controlling the ambient-pressure crystallization by the seeds obtained in the 0.4–0.8 GPa range was demonstrated for GABA monohydrate.<sup>[6]</sup>

Presently we report a simple method of high-entropy nucleation, capable of generating new polymorphs, in this case study on bis-3-nitrophenyl disulphide (3-NO<sub>2</sub>-PhS)<sub>2</sub>, shown on Fig. 1. The thermodynamic conditions of such a nucleation process are extended by subjecting a compound (or its solution) to high-pressure. It increases the range of accessible temperature beyond the ambient-pressure boiling point of the compound (or the solvent), where strongly excited states of rota-vibrations, high-energy conformations, tautomers or other forms not accessible at normal conditions are activated.

The family of biphenyl disulphides is important due to their applications as drugs,<sup>[15]</sup> sensors,<sup>[16]</sup> lubricants,<sup>[17]</sup> polymers,<sup>[18–21]</sup> source of PhS substituents in organic reactions<sup>[22,23]</sup> and precursors for supramolecular systems.<sup>[24–26]</sup> Recently we showed that di-*p*-tolyl disulphide (4-CH<sub>3</sub>-PhS)<sub>2</sub> absorbs the energy of compression by phase transitions and conformational transformations.<sup>[27]</sup> We also observed that exchange reaction between aryl homodimeric disulphides can be achieved at high-pressure without an addition of catalyst. Particularly the reaction between bis-4-chlorophenyl disulphide (4-Cl-PhS)<sub>2</sub> and bis-2-nitrophenyl disulphide (2-NO<sub>2</sub>-PhS)<sub>2</sub> yields a low-density polymorph A of 4-Cl-PhSSPh-2-NO<sub>2</sub> at high-pressure conditions (refcode ROVWUX),<sup>[28]</sup> whereas the catalyst-promoted ball mill liquid-assisted grinding (LAG) at ambient pressure leads to the high-density polymorph (FUQLIM).<sup>[29–30]</sup> The 3-NO<sub>2</sub> analogue, of those disulphides is known, and commercially available in the centrosymmetric form of monoclinic space group C2/c, with molecules located on the 2-fold axes (FUGQUT, hereafter referred to as polymorph  $\alpha$ ).<sup>[31]</sup> Our systematic study on (3-NO<sub>2</sub>-PhS)<sub>2</sub> combines the effects of primary nucleation with dynamic and kinetic crystallization attainable and conveniently controlled under high pressure. We found that the high-entropy nucleation yields two new polymorphs, labelled  $\beta$  and  $\gamma$ , both of lower density as compared to that of polymorph  $\alpha$  obtained at the ambient conditions. The counterintuitive result sheds new light on empirical Ostwald's rule of stages

[a] S. Sobczak, P. Ratajczyk, Prof. A. Katrusiak  
Department of Materials Chemistry  
Faculty of Chemistry  
Adam Mickiewicz University  
Uniwersytetu Poznańskiego 8, 61-614 Poznań (Poland)  
E-mail: katran@amu.edu.pl

[\*\*] A previous version of this manuscript has been deposited on a preprint server (<https://doi.org/10.26434/chemrxiv.13161956.v1>).

 Supporting information and the ORCID identification number(s) for the author(s) of this article can be found under:  
<https://doi.org/10.1002/chem.202005121>.

 © 2021 The Authors. Published by Wiley-VCH GmbH. This is an open access article under the terms of the Creative Commons Attribution Non-Commercial NoDerivs License, which permits use and distribution in any medium, provided the original work is properly cited, the use is non-commercial and no modifications or adaptations are made.

and Wallach's rule relating the densities of enantiomers and racemates.

The protocol for obtaining kinetic polymorphs  $\beta$  and  $\gamma$  resulting from the high-pressure nucleation, described in detail in Supporting Information, was developed in the course of reiterated experiments for different solvents and concentrations. The diamond anvil cell (DAC) chamber was loaded with controlled amounts of  $\alpha$ -(3-NO<sub>2</sub>-PhS)<sub>2</sub> and a solvent. After sealing the DAC, the sample was compressed, and heated until all crystals dissolved. The high-temperature high-pressure nucleation in the DAC was followed by its cooling and opening, aimed at growing the crystals. The quality and size of the crystals recovered from the DAC chamber (of about 0.02 mm<sup>3</sup> in volume) were just sufficient for the single-crystal X-ray diffraction experiments, solution and refinement of the structures, although due to the small size of the samples the reflections were weak, which affected the range of  $2\theta$  angle for observed reflections and the accuracy of refined parameters (see the Supporting Information).

Well known are the structural features usually valid for the polymorphs obtained under kinetic regime: (i) their symmetry is lower,<sup>[32]</sup> (ii) their  $Z'$  number is higher,<sup>[3,32–34]</sup> and (iii) they are less dense, when compared to the dynamic-regime polymorphs.<sup>[35]</sup> It is also characteristic of conformational polymorphs that (iv) the kinetic polymorphs are built of conformers of the potential energy ( $E_p$ ) higher than those of the dynamic polymorphs.<sup>[5,9,36,37]</sup>

Both polymorphs  $\beta$  and  $\gamma$  of (3-NO<sub>2</sub>-PhS)<sub>2</sub> could be textbook examples of kinetic polymorphs, with all their characteristic features (i–iv). Both forms crystallize in the chiral space group  $P2_1$ , which is a subgroup of space group  $C2/c$ , and their density is significantly lower than that of polymorph  $\alpha$  (Table 1). It is remarkable that the structures of both polymorphs  $\beta$  and  $\gamma$  are composed of layers displaying a pseudo-symmetry involving local inversion centres and glide planes perpendicular to  $[y]$ . In polymorph  $\beta$  the pseudo-inversion lies at [0.195, 0.13, 0.24]; in polymorph  $\gamma$  the pseudo-inversion is at [0.38, 0.11, 0.23] and the pseudo-glide planes are perpendicular to  $[y]$  and parallel to the layers (cf. Figure S4 in Supporting Information).

As illustrated in Figure 1, the disulphide molecules are conformationally flexible and their 'soft' torsion angles about bonds S–S ( $\tau$ ) and C–S ( $\tau_2$  and  $\tau_3$ ) can be modified by momentary environment changes in the liquid and by crystal field in

Polymorph	$\alpha$ <sup>[31]</sup>	$\beta$	$\gamma$
space group	$C2/c$	$P2_1$	$P2_1$
$a$ [Å]	13.6731(9)	8.1262(17)	8.1069(10)
$b$ [Å]	8.9078(6)	26.952(4)	22.406(3)
$c$ [Å]	12.4539(8)	12.6335(19)	14.7478(16)
$\beta$ (°)	120.070(1)	105.214(19)	94.087(12)
$V$ (Å <sup>3</sup> )	1312.70(15)	2669.9(8)	2672.0(6)
$Z/Z'$	4/0.5	8/4	8/4
$V/Z$	328.18	333.74	334.01
$D_x$ (g/cm <sup>3</sup> )	1.573	1.534	1.533

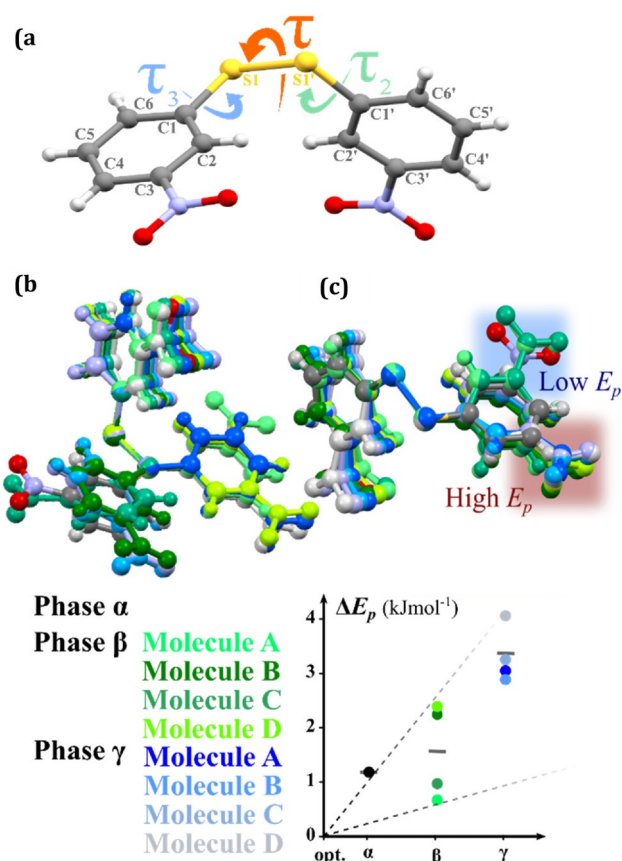


**Figure 1.** Conformers in (3-NO<sub>2</sub>-PhS)<sub>2</sub> (a) polymorph  $\alpha$  with torsion angles  $\tau$ ,  $\tau_2$  and  $\tau_3$  indicated; (b) all molecules of polymorphs  $\alpha$ ,  $\beta$ , and  $\gamma$  superimposed on the C1-S1-S1' fragment; (c) these rotational enantiomers adjusted to torsion angle  $\tau$  positive in order to visualise the presence of low- $E_p$  and high- $E_p$  conformers. The plot shows the  $E_p$  differences and bars indicate their average values.

the solid state. The  $Z'$  number is 0.5 in dynamic polymorph  $\alpha$ , hence its torsion angles  $\tau_2$  and  $\tau_3$  are identical, while in kinetic polymorphs  $\beta$  and  $\gamma$  the  $Z'$  number is 4. In polymorph  $\beta$  four independent conformers, labelled A, B, C and D, are located at general positions, in pseudo-centrosymmetric relations between conformers A to C, and B to D. This relation is most prominent for torsion angles  $\tau$ ,  $\tau_2$  and  $\tau_3$  (Table 2). Similar pseudo-symmetry relations are also apparent in the structure of polymorph  $\gamma$ .

The (3-NO<sub>2</sub>-PhS)<sub>2</sub> molecule has two favoured conformations. In the low- $E_p$  (LE) conformer angles  $\tau$ ,  $\tau_2$  and  $\tau_3$  are close to 90°, 0° and 0°, whereas in the high- $E_p$  (HE) conformer these angles are close to 90°, 0° and 165°, respectively. Polymorph  $\alpha$  is built of LE conformers (Figure 1 and Table 2), in polymorph  $\beta$  there are equal numbers of LE and HE conformers; in polymorph  $\gamma$  only HE conformers are present. The average conformational energies of polymorph  $\alpha$ ,  $\beta$ , and  $\gamma$  are 1.18, 1.57 and 3.42 kJ mol<sup>-1</sup> (referred to the fully optimized low-energy conformer) as shown in the inset in Figure 1. Polymorphs  $\beta$  and  $\gamma$  (Figure 2) contain equal numbers of rotational enantiomers and in this respect they are conformational kryptoracemates.<sup>[38]</sup>

**Table 2.** Torsion angles  $\tau_1$ ,  $\tau_2$  and  $\tau_3$  (Figure 1) in conformers present in (3-NO<sub>2</sub>-PhS)<sub>2</sub> polymorphs  $\alpha$  (half molecule independent),  $\beta$  and  $\gamma$  (4 independent molecules labelled A, B, C and D), as well as their potential energy  $\Delta E_p$  related to the fully optimized isolated conformer. LE denotes low  $E_p$  and HE high  $E_p$  conformers.

Torsion angle	$\tau_1$ [°]	$\tau_2$ [°]	$\tau_3$ [°]	$\Delta E_p$ [kJ mol <sup>-1</sup> ]	$E_p$ state
optimized mol.	84.78	4.13	4.13	0	LE
phase $\alpha$	97.63	-8.55	-8.55	1.18	LE
phase $\beta$	A	-88.07	-22.32	12.06	LE
	B	87.08	-1.24	171.13	HE
	C	91.21	-14.30	21.27	LE
	D	-87.01	1.46	-169.62	HE
phase $\gamma$	A	-84.77	-5.30	-162.45	HE
	B	91.05	8.26	163.13	HE
	C	89.39	16.49	165.05	HE
	D	-91.05	-22.65	-165.42	HE

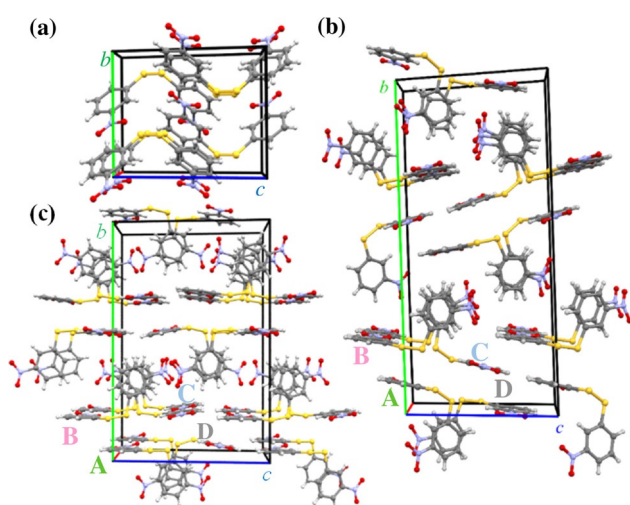


**Figure 2.** Structure of (3-NO<sub>2</sub>-PhS)<sub>2</sub> polymorphs (a)  $\alpha$ ; (b)  $\beta$ ; and (c)  $\gamma$ . Capital letters A, B, C and D label independent conformers in polymorphs  $\gamma$  and  $\beta$ .

Apart from the molecular conformation, the crystal structure and packing motifs in polymorph  $\alpha$  of (3-NO<sub>2</sub>-PhS)<sub>2</sub> strongly differ from those in isomers (2-NO<sub>2</sub>-PhS)<sub>2</sub> (ODNPDS)<sup>[39]</sup> and (4-NO<sub>2</sub>-PhS)<sub>2</sub> (NIPHSS).<sup>[40]</sup> In their crystals, molecules are linked into chains by C–H...O hydrogen bond, absent in  $\alpha$ -(3-NO<sub>2</sub>-PhS)<sub>2</sub>, where sheets are formed through  $\pi$ - $\pi$  stacking of aromatic rings.<sup>[31,41]</sup> On the other hand, in (3-NO<sub>2</sub>-PhS)<sub>2</sub> polymorphs  $\beta$  and  $\gamma$  various types of intermolecular contacts (Figure S2) and cohesion forces are present, such as CH...O,  $\pi$ - $\pi$  stacking and S...S.

It is apparent that the conditions of nucleation affect the hierarchy of interactions in the crystal structure. It was demonstrated that the intermolecular hydrogen bonds are strongly modified under pressure,<sup>[42–44]</sup> when they have to compromise with the increased role of close packing. Most importantly, ambient-pressure molecular crystals easily sublime, melt and evaporate, but under high-pressure the temperature of the system can be increased to higher values, which increases the kinetic energy of molecular motion. According to Boltzmann's statistics for the ideal gas, the average kinetic energy of its

molecules increases linearly with temperature and is equal  $k_B T/2$  ( $k_B$  is Boltzmann's constant) per each degree of freedom. This rough assessment, when applied to molecules of (3-NO<sub>2</sub>-PhS)<sub>2</sub>, shows that high temperature can easily destabilize their interactions (mainly C–H...O, Figure S2) and excite the conformers to the HE states, then observed in polymorphs  $\beta$  and  $\gamma$ . The increased  $E_p$  values of conformers in these high- $T/p$  polymorphs (Table 2) increase their chemical potential, compared to that of polymorph  $\alpha$ .<sup>[45,46]</sup>

Thus, the internal energies ( $U$ ) of polymorphs  $\beta$  and  $\gamma$  are higher compared to that of polymorph  $\alpha$ . This  $U$ -energy relation is essential for the most surprising high average volume of molecules in polymorphs  $\beta$  and  $\gamma$ , as their crystal fields stabilize the HE conformers (Tables 1 and 2). At first glance, this result seems to contradict numerous high-pressure crystallizations and syntheses leading to high-density polymorphs. In fact, high-pressure techniques are generally aimed at obtaining hard, high-density forms of crystals.<sup>[47]</sup> However, such crystallizations are performed slowly under the dynamic regime, allowing the system to equilibrate. All characteristic features (i–iv) of kinetic polymorphs can be rationalized in terms of the thermodynamic conditions of the crystallization process: (i) the low symmetry is a consequence of the conformational and orientational variety consistent with the high entropy of the system at high-temperature, which is also connected with (ii) the high  $Z'$  number; the high  $T$  also explains the high  $E_p$  states of excited molecules (compared to lower  $E_p$  conformer in the dynamic polymorph  $\alpha$ ). The quick crystallization leaves no sufficient time for the molecules to reorient or change the positions of substituents. Finally, the low density (iii) despite the high-pressure conditions can be attributed to: (a) higher internal energy, in part associated with the HE conformers and the cohesion forces partly used for their stabilization; (b) higher compressibility of the low-density polymorphs than that of the high-density polymorph, hence their density difference diminishes with pressure; (c) the nucleation taking place at high temperature implies high entropy and strong rota-vibrations requiring an additional space; and (d) the high-temperature nucleation directs the crystallization leaving no space for other polymorphs, particularly that the crystallization is the fastest close to the melting curve.

It is convenient to heat sample under pressure, which increases the freezing point and hence moves the nucleation to the high-entropy region. Furthermore, under high-pressure the viscosity of the solution or melt significantly increases,<sup>[48]</sup> which hampers the rigid-molecule motions and internal reorientations of molecular moieties. These effects of viscosity are thus consistent with varied conformations and high  $Z'$  number. Moreover, the increased viscosity expands the time scale for the kinetic crystallization. In other words, the kinetic process at high-pressure is considerably slower than at 0.1 MPa. This 'extended' kinematic regime increases the likelihood of the nucleation of kinetic polymorphs. Then the growth of their seeds is favourably continued on lowering the temperature, which reduces the concentration of the solution to below the saturation and prevents the nucleation of other polymorphs, even when the process is slowed down to the dynamic regime.

Interestingly, all our attempts to obtain the kinetic polymorphs  $\beta$  and  $\gamma$  by mechanochemical methods, liquid-assisted grinding (LAG) with acetonitrile and isopropanol, as well as neat ball milling, failed (*cf.* Supporting Information). This contrasts with the successful production of heterodimeric low-density polymorph A of 4-Cl-PhSPh-2-NO<sub>2</sub> during the neat grinding.<sup>[28,29]</sup> Later, we obtained this polymorph by high-entropy nucleation, too.<sup>[27]</sup>

To conclude, the high-pressure crystallization of low-density polymorphs  $\beta$  and  $\gamma$  of (3-NO<sub>2</sub>-PhS)<sub>2</sub> reveals the background of this counterintuitive phenomenon. The increased pressure expands the thermodynamic space of temperature and concertation, where high-entropy nucleation is the source of kinetic polymorphs. The molecular-level mechanism of Ostwald's rule of stages appears as a natural consequence of the kinetic effects fueled by the considerably increased accessible temperature range under high pressure. Noteworthy, (3-NO<sub>2</sub>-PhS)<sub>2</sub> low-density polymorphs  $\beta$  and  $\gamma$  are non-centrosymmetric, unlike the centrosymmetric polymorph  $\alpha$ . Centrosymmetric crystals are usually more dense than non-centrosymmetric ones, but rare exceptions from this rule<sup>[49,50]</sup> can be regarded as an indication that more experimental results and studies are needed for the rigorous description of the crystallization process, which still today is often considered to be more 'art' than 'science'.<sup>[1]</sup>

### Supporting Information

Detailed experimental data including protocol for obtaining high-pressure nucleated polymorphs, single-crystals of polymorphs  $\beta$  and  $\gamma$ , the shortest intermolecular contacts plotted for all polymorphic forms, A, B, C and D conformers present in form  $\beta$  and  $\gamma$  together with their pseudo-symmetry relations, as well as the results of ball-mill experiments can be found in Supporting Information. Deposition Number(s) 2040892 and 2040891 contain(s) the supplementary crystallographic data for this paper. These data are provided free of charge by the joint Cambridge Crystallographic Data Centre and Fachinformationszentrum Karlsruhe Access Structures service [www.ccdc.cam.ac.uk/structures](http://www.ccdc.cam.ac.uk/structures).

### Acknowledgements

We thank the Polish National Science Centre (grant PRELUDIUM 2017/27/N/ST5/00693) for financial support. This research was supported in part by PLGrid Infrastructure.

### Conflict of interest

The authors declare no conflict of interest.

**Keywords:** crystal growth · high-pressure chemistry · kinetic crystallization · nucleation · polymorphism

[1] J. Bernstein, *Polymorphism in Molecular Crystals*, Oxford University Press, 2007.

- [2] J. Bernstein, *J. Phys. D* **1993**, *26*, B66–B76.  
 [3] J. Bernstein, J. D. Dunitz, A. Gavezzotti, *Cryst. Growth Des.* **2008**, *8*, 2011–2018.  
 [4] R. J. Davey, N. Blagden, G. D. Potts, R. Docherty, *J. Am. Chem. Soc.* **1997**, *119*, 1767–1772.  
 [5] A. Nangia, *Acc. Chem. Res.* **2008**, *41*, 595–604.  
 [6] F. P. A. Fabbiani, G. Buth, D. C. Levendis, A. J. Cruz-Cabeza, *Chem. Commun.* **2014**, *50*, 1817–1819.  
 [7] S. M. Woodley, R. Catlow, *Nat. Mater.* **2008**, *7*, 937–946.  
 [8] A. R. Oganov, *Modern Methods of Crystal Structure Prediction*, **2010**.  
 [9] S. L. Price, *Phys. Chem. Chem. Phys.* **2008**, *10*, 1996–2009.  
 [10] A. Gavezzotti, *Acc. Chem. Res.* **1994**, *27*, 309–314.  
 [11] J. Halebian, W. McCrone, *J. Pharm. Sci.* **1969**, *58*, 911–929.  
 [12] F. P. A. Fabbiani, D. R. Allan, S. Parsons, C. R. Pulham, *Acta Crystallogr. Sect. B* **2006**, *62*, 826–842.  
 [13] K. F. Dziubek, A. Katrusiak, *J. Phys. Chem. B* **2004**, *108*, 19089–19092.  
 [14] B. A. Zakharov, S. V. Goryainov, E. V. Boldyreva, *CrystEngComm* **2016**, *18*, 5423–5428.  
 [15] J. M. Young, A. J. Tomolonis, *Agents Actions* **1987**, *21*, 314–315.  
 [16] M. B. Gholivand, Y. Mozaffari, *Talanta* **2003**, *59*, 399–407.  
 [17] E. S. Forbes, *Wear* **1970**, *15*, 87–96.  
 [18] S. Nevejans, N. Ballard, J. I. Miranda, B. Reck, J. M. Asua, *Phys. Chem. Chem. Phys.* **2016**, *18*, 27577–27583.  
 [19] J. M. Matxain, J. M. Asua, F. Ruipérez, *Phys. Chem. Chem. Phys.* **2016**, *18*, 1758–1770.  
 [20] E. Formoso, J. M. Asua, J. M. Matxain, F. Ruipérez, *Phys. Chem. Chem. Phys.* **2017**, *19*, 18461–18470.  
 [21] M. Irigoyen, J. M. Matxain, F. Ruipérez, *Polymers (Basel)* **2019**, *11*, 1960.  
 [22] J. H. Byers, *Encycl. Reagents Org. Synth.*, American Cancer Society **2001**.  
 [23] T.-L. Ho, M. Fieser, L. Fieser, *Fieser Fieser's Reagents Org. Synth.*, John Wiley & Sons, Inc., Hoboken, NJ, USA **2006**.  
 [24] S. P. Black, J. K. M. Sanders, A. R. Stefankiewicz, *Chem. Soc. Rev.* **2014**, *43*, 1861–1872.  
 [25] T. Friščić, *Chem. Soc. Rev.* **2012**, *41*, 3493–3510.  
 [26] N. M. Phan, E. G. Percástegui, D. W. Johnson, *Chempluschem* **2020**, *85*, 1270–1282.  
 [27] S. Sobczak, A. Katrusiak, *J. Phys. Chem. C* **2017**, *121*, 2539–2545.  
 [28] S. Sobczak, W. Drożdż, G. I. Lampronti, A. M. A. Belenguer, A. Katrusiak, A. R. Stefankiewicz, *Chem. Eur. J.* **2018**, *24*, 8769–8773.  
 [29] A. M. Belenguer, G. I. Lampronti, D. J. Wales, J. K. M. Sanders, *J. Am. Chem. Soc.* **2014**, *136*, 16156–16166.  
 [30] A. M. Belenguer, T. Friščić, G. M. Day, J. K. M. Sanders, *Chem. Sci.* **2011**, *2*, 696.  
 [31] D. Cannon, C. Glidewell, J. N. Low, J. L. Wardell, *Acta Crystallogr. Sect. C* **2000**, *56*, 1267–1268.  
 [32] J. W. Steed, *CrystEngComm* **2003**, *5*, 169–179.  
 [33] C. P. Brock, *Acta Crystallogr. Sect. B* **2016**, *72*, 807–821.  
 [34] K. M. Steed, J. W. Steed, *Chem. Rev.* **2015**, *115*, 2895–2933.  
 [35] E. H. Lee, *Asian J. Pharm. Sci.* **2014**, *9*, 163–175.  
 [36] S. L. Price, *Acta Crystallogr. Sect. B* **2013**, *69*, 313–328.  
 [37] A. J. Cruz-Cabeza, S. M. Reutzel-Edens, J. Bernstein, *Chem. Soc. Rev.* **2015**, *44*, 8619–8635.  
 [38] L. Fábrián, C. P. Brock, *Acta Crystallogr. Sect. B* **2010**, *66*, 94–103.  
 [39] C. Glidewell, J. N. Low, J. L. Wardell, *Acta Crystallogr. Sect. B* **2000**, *56*, 893–905.  
 [40] J. S. Ricci, I. Bernal, J. S. Ricci, I. Bernal, *J. Am. Chem. Soc.* **1969**, *91*, 4078–4082.  
 [41] C. Glidewell, J. N. Low, J. M. S. Skakle, J. L. Wardell, *Acta Crystallogr. Sect. C* **2002**, *58*, o485–o486.  
 [42] E. Patyk, J. Skumiel, M. Podsiadlo, A. Katrusiak, *Angew. Chem. Int. Ed.* **2012**, *51*, 2146–2150; *Angew. Chem.* **2012**, *124*, 2188–2192.  
 [43] M. Podsiadlo, A. Olejniczak, A. Katrusiak, *CrystEngComm* **2014**, *16*, 8279–8285.  
 [44] K. W. Rajewski, M. Andrzejewski, A. Katrusiak, *Cryst. Growth Des.* **2016**, *16*, 3869–3874.  
 [45] P. Dopieralski, J. Ribas-Arino, P. Anjukandi, M. Krupicka, J. Kiss, D. Marx, *Nat. Chem.* **2013**, *5*, 685–691.  
 [46] P. Dopieralski, J. Ribas-Arino, P. Anjukandi, M. Krupicka, D. Marx, *Nat. Chem.* **2017**, *9*, 164–170.  
 [47] E. Boldyreva, *Cryst. Growth Des.* **2007**, *7*, 1662–1668.

- [48] E. U. Franck, *Experimental Studies of Compressed Fluids in High Press. Chem. Biochem.*, Springer Netherlands, Dordrecht, **1987**, pp. 93–116.
- [49] W. Cai, J. Marciniak, M. Andrzejewski, A. Katrusiak, *J. Phys. Chem. C* **2013**, *117*, 7279–7285.
- [50] J. Marciniak, M. Andrzejewski, W. Cai, A. Katrusiak, *J. Phys. Chem. C* **2014**, *118*, 4309–4313.

---

Manuscript received: November 26, 2020

Revised manuscript received: January 18, 2021

Accepted manuscript online: January 28, 2021

Version of record online: March 4, 2021

---